NANOMAGNETITE ENHANCED PARAFFIN FOR THERMAL ENERGY STORAGE APPLICATIONS

F. R. SAEED[a], E. C. SERBAN[a], E. VASILE[b], M.H.A.A. AL-TIMIMI[a], W. H. A. AL-BANDA[a], M. Z. A. ABDULLAH[a], I. STAMATIN[a], A. CUCU[a], S. M. IORDACHE[a], S. VOINEA[a], A. E. BALAN[a*]
[a] *University of Bucharest, Faculty of Physics, 3Nano-SAE Research Centre, 405 Atomistilor str., PO Box MG-38, Bucharest-Măgurele, Romania*
[b]*Politehnica University of Bucharest, 313 SplaiulIndependentei, Bucharest, Romania*

Phase change materials (PCMs), i.e. materials that store and release thermal energy loads during phase transitions, have found direct applications in thermal energy storage and thermal management of electronic devices. Paraffin wax constitutes a popular PCM due to its chemical stability (as an alkane) and considerable latent heat; however, paraffin's thermal performance (e.g. thermal conductivity) has posed consistently as a problem in its further realization as a PCM. To address this, an experimental study is conducted in order to determine the effect of adding Fe_3O_4 nanoparticles on paraffin thermal performances. The metallic nanoparticles were synthesized by co-precipitation method and added in 1-10 wt. % ratios to paraffin. Thermal behaviour in terms of melting and solidification temperatures/ enthalpies and specific heat capacities of solid and liquid paraffin composites was determined by differential scanning calorimetry (DSC). Moreover, the activation energies of Fe_3O_4 nanoparticle/PCM were estimated using Kissinger method. Results show a modification of the activation energy of solid-solid and solid-liquid transitions for the nanocomposites compared to pristine paraffin and a latent heat enhancement for the 5 wt.% Fe_3O_4 loading, while the melting temperature range remained the same. The presented results make the Fe_3O_4 nanoparticle a good candidate to be used for thermal behaviour improvement of thermal energy storage applications.

(Received February 2, 2017; Accepted April 7, 2017)

Keywords: Phase change material (PCM), Paraffin, Nanoparticle-enhancement, Thermal performance

1. Introduction

Thermal energy storage through latent heat is one of the most important applications of renewable energy storage [1-2].The storage of thermal energy can categorized as three essential parts, latent heat, sensible heat and chemical heat. Latent heat storage system is based on thermal energy storage at the phase transition temperature from solid to liquid phase. The vital role of this facility is the selection a specific PCM for a particular application depend primarily at which on melting temperature range (phase change) of that PCM. Due to the suitable properties of the paraffin such as stability, noncorrosive, and nontoxic can consider a good options for using as PCM. The drawback that associated with utilizing of paraffin as PCM is the low thermal conductivity[3].

Various techniques were used to overcome the issue in the thermal performance of PCM such as brushes, fines, metal foam, and fine particles. When nano-graphite (NG) is mixed with paraffin a random orientation dispersion was found, with a heat transmission enhanced which hence amended the energy storage technology [4]. From feasibility side, NG price is low and the improvement of NG in thermal conductivity was exceptional. Furthermore, latent heat had decreased with increasing of NG content, slight influence on the melting point of the paraffin was

* Corresponding author: andronie@3nanosae.org

noticed. Multi-walled carbon nanotubes (MWCNTs) dispersed in 1-dodeconal with a concentration of 0 wt%, 1 wt%, and 2 wt% were also studied [5].Although, heat conduction was intensified due to dispersion of nanoparticles, the viscosity was increased under the effect of decreasing buoyancy-driven natural convection. Melting was shown to be decelerated for two weight concentrations of nanoparticles loadings as the degradation in natural convection (results from viscosity augmentation) exceeded the enhancement in conduction (due to increase in thermal conductivity). Furthermore, the experimental results were in contrast to the documented numerical results where an acceleration of melting was achieved.

Another approach is to improve the thermal conductivity and shape stability of paraffin by adding exfoliated graphite nanoplatelets (xGnP)[6]. At 10% of x GnP thermal conductivity increased by more than 10 times. The low cost of x GnP and high thermal conductivity make it appropriate selection for PCM applications. The effect of various volume fraction of inverse micelles on the thermal properties during melting and freezing of n-hexadecane have been studied also [7].A thermal conductivity enhancement of dioctyl sodium sulfosuccinate, oleic acid, and sorbitan at the phase transition between the solid and liquid phases was about 185, 119, and 111%, for the inverse micelles size ∼1.5−6 nm has been reported. Results suggested that while the first-order phase transition, the highly packed linear chain surfactant of the inverse micelles are pushed to the inter crystal boundaries of alkanes, therefor it lead to the decreasing the interfacial thermal resistance.

The addition of Cu, Al, and C/Cu nanoparticles to the melting paraffin resulted in increased thermal conductivity, with a decrease in the rate of heating and cooling by 30.3% and 28.2% for 1wt % of Cu/ paraffin composite, respectively[8]. Another study showed that the thermal conductivity ofP CM and the charging and discharging time of LTES has also been reduced significantly when dispersingCuOnanoparticleswithinthe PCM[9]Al_2O_3 nanoparticles have been considered also as nanoparticles embedded in paraffin [10]. It was found that a little effect of melting/ freezing behavior of PCM due to the addition of 5wt% and 10wt% respectively of Al_2O_3 nanoparticles. From the side of effective thermal conductivity the detected non-liner behavior with the weight fraction had been detected, relative promote was found with temperature raising. Another study regarding the melting of solid–liquid phase-change material (n-octadecane) with dispersed Al_2O_3 nanoparticles concluded that the natural convection-dominated heat transfer rate across the melted region and thus the total energy transfer into the enclosure tend to degrade greatly with increasing mass fraction of the nanoparticles[11]. They reasoned this degradation as the enhancement in the thermal conductivity of the nano-PCM due to dispersing the Al_2O_3 nanoparticles could be outweighed by the far greater enhancement in the dynamic viscosity of the liquid nano-PCM.

Another material employed as additive is the nano-magnetite (Fe_3O_4) for paraffin composites with enhanced thermal conductivity[12]. Sol-gel method was used for nanomagnetite preparation and mixed with paraffin in10% and 20% mass fraction. The results showed, increasing in thermal conductivity by 48% and 67% for 10% and 20% of nanomagnetite for the PNMC. On the other hand it was noticed a slight improvement in latent heat capacity while the melting temperature of the composite was stable. After 500 cycles, of thermal stability test, it was not found any change in thermal storage capacity.

Therefore, authors aim to investigate the effects of Fe_3O_4 nanoparticle on thermal properties of paraffin, benefiting from its high thermal conductivity of about 100W/m K [13]. Although a considerable amount of data are available, the above mentioned studies have not yet led to a detailed understanding of the role of the nanoparticles in modifying thermal behaviour of paraffin based materials. With this purpose, Fe_3O_4 nanoparticles were synthesized by co-precipitation method and added in 1-10 wt. % ratios to paraffin. The effect of the Fe_3O_4 nanoparticle mass fraction on the effective thermal properties including phase change temperatures, latent heat and activation energies of the prepared PCM have been investigated. Additionally, the activation energy of the phase transitions are also estimated using Kissinger model.

2. Experimental

2.1. Synthesis of Fe_3O_4

Nanomagnetite Fe_3O_4 were synthesized by chemical precipitation method[14], which achievedby co-precipitation of 2:1 molar ratio of ferric and ferrous ions (Fe^{+3}: Fe^{+2}). 1.625g of ferric chloride $FeCl_3$ were dissolved in 30 ml of 2M HCl in a beaker, and0.995 g of ferrous chloride $FeCl_2.4H_2O$ was dissolved in 30 ml of 2M HCl in a second beaker.The solutions were mixed together and stirred for 15 minutes at 1200 rpm.60 ml of 5 M NaOH (99% purity)- reducing agent were added to the solution dropwise while stirring at 1200 rpm until precipitation the black magnetite powder of Fe_3O_4.The reducing time was about 4 minutes and the pH adjusted at 11.The co-precipitate powder was washed with distillate water for several times until neutral pH. Centrifuge was used for washing at 6000 rpm for 20 minute for each washing process. The powderwas dried in an air ovenfor 24 hour at 50^{o}C.

2.2. Preparation of paraffin / Fe_3O_4nanoparticles mixture

The mixture of paraffin/ Fe_3O_4 was prepared by melting the paraffin (RT58, Sigma Aldrich) at 70^{o}C for 30minutes and then adding the Fe3O4 nanoparticles to the liquid paraffin in different concentrations: 1%, 5% and 10%wt.The nanoparticles were dispersed in the solution for 30 minutes using an ultrasonic bath.

2.3. Characterization methods

Scanning electron microscope (SEM) coupled with EDAX(JIB-4600F) had been used for testing the Fe_3O_4particles. FT-IR Spectroscopy was performed by FT-IR Jasco Spectrometer, model 6200 in the range 4000-400 cm^{-1}, resolution 0.4 cm^{-1}.Thermal analysis are performed by means of differential scanning calorimeter (DSC Mettler Toledo, model Star1) in nitrogen atmosphere at heating rates of 5, 10, 15, 20 and 25^{o}C/min in the temperature range 20-90^{o}C. The 5-10 mg samples are sealed in aluminium pans. DSC curves were analysed with DSC Standard Data Analysis Program associated with model Star1. Indium was used as a calibration reference of DSC. Each sample treated for 30 min at 90^{o}C to lose the thermal memory effect.

3. Results and discussions

3.1. Scanning electron microscopyand EDX

Nanoparticle typical morphology can be observed in Fig. *1*, the shape of the Fe_3O_4 particles are nearly spherical and the size distribution is almost homogenous. The size of the obtained Fe_3O_4 nanoparticles are in range of 16.6 – 30.1 nm.

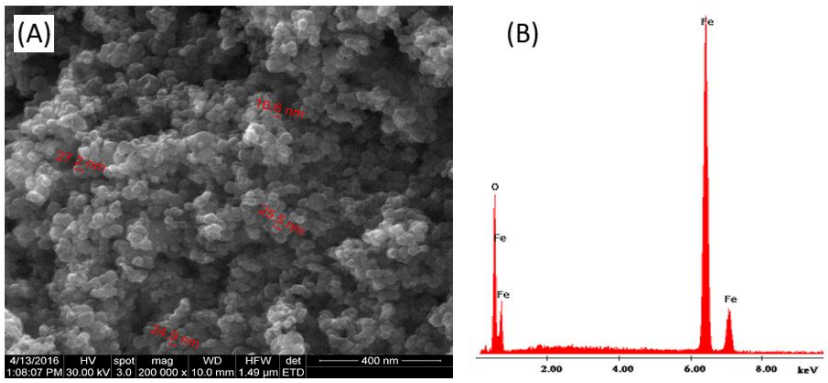

Fig. 1. (A) SEM image and (B) EDX test of Fe_3O_4nano-magnetite.

EDX analysis showing the composition of Fe_3O_4-nanomagnetite sample is presented in Fig. 1(B). The analysis confirm the presence of pureFe_3O_4 on various regions. Other elements notrelated to the structure of the nanomagnetite Fe_3O_4 were not detected.

3.2. FTIR Spectroscopy

The FT-IR spectrum of the Fe_3O_4-nanomagnetite sample is shown in

Fig. *2*. The maximum density correspond to the presence of Fe-O bond which is in the lattice crystalline of Fe_3O_4 found at 570 cm^{-1}[15]. The detect peak represented the characterization peak that appear in the metal oxides and is associated with the structure vibration of the metal octahedral and tetrahedral [16]. The peak at 1645 cm^{-1} represent the H-O-H bending vibration, as a detection for the H_2O molecule. The presence for this peak is a result for water absorption from the surface of the nanoparticles. Also a stretching and bending vibration of the O-H corresponds to the peak at 1393cm^{-1}[12]. The remains of basic solution that used in the synthesis method may interpret the reason for the presence of the OH peak of the analysis [17].

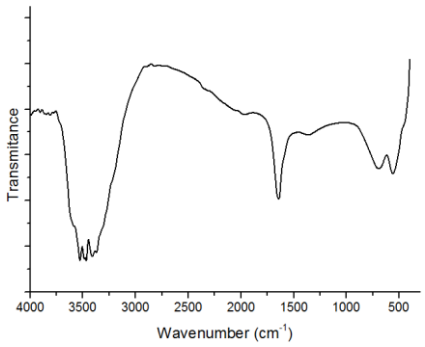

Fig. 2. FTIR spectra of Fe_3O_4

3.3. Thermal analysis

Thermal behaviour of paraffin with different loadings of Nano-magnetite (Np-0, Np-1, Np-5 and Np-10) with the heating and cooling rate of 10K/min is shown in Figure 3, where few specific features are distinguished: solid-solid and solid-liquid phase transitions [18].The solid-solid transition is a property of some paraffin waxes prior to isotropizationof the melt, which occurs due to a monoclinic crystal disordering to a pseudohexagonal crystal. The changes in the melting and solidification temperature are associated to the nanoparticles presence in the mixture and the different concentrations of these nanoparticles.

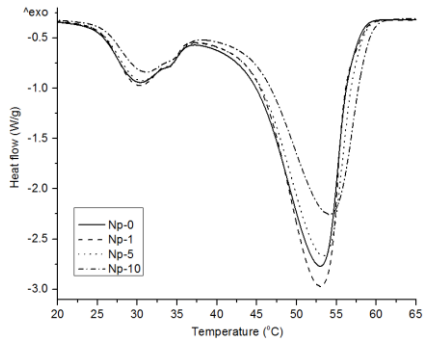

Fig. 3. DSC thermograms of paraffin with different loadings of Fe_3O_4- nanoparticles (Np-0, Np-1, Np-5 and Np-10) with the heating and cooling rate of 10^oC/min.

However the variation in the melting and freezing points is not remarkable under the various loading of nanoparticles effect as shown inTable 1. The enthalpy of PCM calculated by

integrating the area under curve. The phase transition of the PCM (melting and solidification) occur over a range of temperatures. The heating, cooling rate and sample size have a signifying effect on the function of the effective heat capacity. The apparent heat capacity can be calculated by obtaining heat flow and heat capacity of the solid or liquid phase of PCM using the following equation:

$$Cp, app(T) = \frac{\emptyset(T)}{mT} + Cp \quad (1)$$

where*m* is the mass of the sample, *T* is the rate of heating or cooling, and $\emptyset(T)$ is the heat flow rate. Fig. *4* (A) shows the sensible and latent heat of phase transition for solid-solid and solid-liquid phase transformation of the paraffin wax and the paraffin/Fe_3O_4 mixture at variousconcentrations.

The heat of fusion seems to be increasedslightly with the nanoparticles increasing of the paraffin/Fe_3O_4 mixture excluding to the 10wt% loading, the lowest heat of fusion found with the paraffin of 10 wt %$Fe_3O_4$and the maximum indicated at 1wt.%of Fe_3O_4loading. The slight enhancement of the latent heat of fusion for 1 and 5wt.% of Fe_3O_4 loading can be interpreted as a result to the enhanced intermolecular interaction due to the ratio of high surface area to the volume of nanoparticles. Another explanation is relevant to surface defect sites caused by various coordination geometry of the Fe_3O_4 structure which improve the surface interaction of the paraffincomposite [12].Similar behaviour of latent heat enhancement of PCMs were recorded for carbon nanotubes and nano-SiO_2mixtures [19-20]. The 1wt.%percent of the nanoparticlescan consider the most suitable concentration to provide the maximum surface interaction between Fe_3O_4 and the surrounding paraffin without an excessive interaction between the nanoparticles themselves which might occur in other ratios.

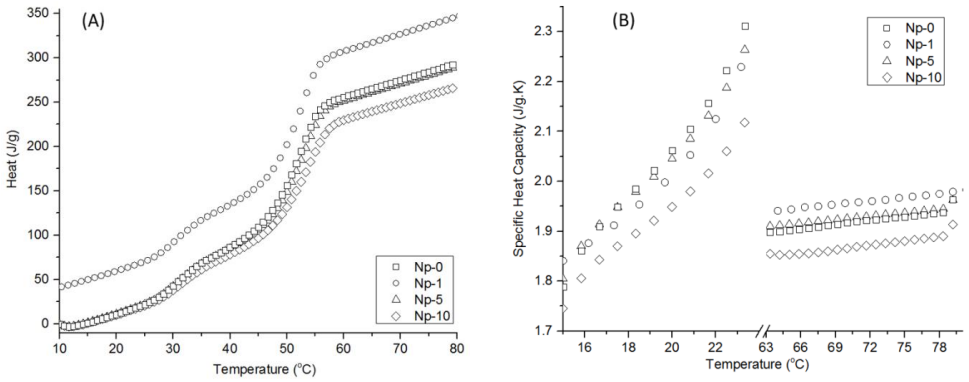

Fig. 4. (A) The sensible and latent heat of phase transition for solid-solid and solid-liquid phase transformation of the paraffin wax and the paraffin/nano-magnetite mixture of different loadings (Np-0, Np-1, Np-5 and Np-10). (B) The impact of the nano-magnetite Fe_3O_4 concentrations on the specific heat capacity for the liquid and solid phases.

Three characterization temperature were determined by the heat flow signal for each transition: the temperature which correspond to the separation of the DSC heat flow from the heating course base (transition temperature), the onset of the melting peak (melting temperature), and temperature compatible to the separation rate of the DSC heat flow curve from the base line in the cooling course (solidification temperature). The melting temperature T_m, transition temperature T_t and total enthalpy change ΔH of the pure paraffin and the mixtures are shown in Table 1.

Table 1. The melting temperature Tm, transition temperature Tt, and total enthalpy change ΔH of the pure paraffin and the mixtures.

Sample	%wt.Fe_3O_4	T_t (^oC)	T_m(^oC)	ΔH(J/g)
Np-0	0.00	24.61	43.72	173.21
Np-1	1.00	25.12	44.66	181.00
Np-5	5.00	25.10	44.23	178.25
Np-10	10.00	25.51	44.54	161.15

Measuring of heat capacity for the paraffin and paraffin/Fe_3O_4composite with various loading of nanoparticles were achieved. Fig. *4* (B) shows the impact of the Fe_3O_4 concentrations on the specific heat capacity for the liquid and solid phases.Table 2 shows the heat capacities of the solid and liquid phase extracted from Fig. *3*. It can be noticed that the specific heat capacity increased gradually with 1, 5 and 10wt.%thatthe maximum value of increasing werecorresponded to the 1wt%and5wt % of the nanoparticles. Also it can be observe that the increasing and decreasing of the specific heat capacity is almost the same for the both phases.

Table 2. Heat capacities of the solid and liquid phase at (s, 15^{o}C) and (l, 80^{o}C).

Sample	Np-0%	Np-1%	Np-5%	Np-10%
Cp (s, 15^{o}C)(J/g.K)	1.62	1.84	1.80	1.75
Cp (l, 80^{o}C) (J/g.K)	1.68	1.98	1.96	1.91

Various values of heating rates were obtained by DSC for each sample which allow to draw the relation between$\ln(V/T_p^2)$ and $1000/T_p$by Kissinger method [21](Figure 5). Curve equation could be expressed by Kissinger method and by the slop value of the curve the activation energy for the sample could be determined. The activation energy, pre-exponential factor, and correlation coefficient are shown in Table 3.

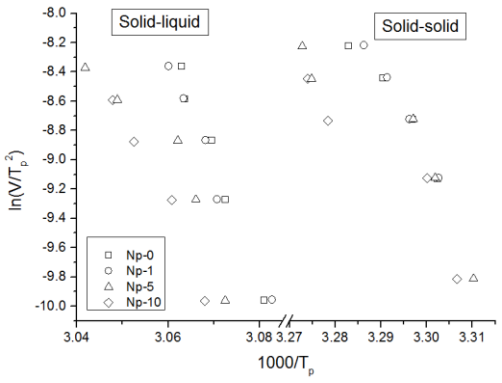

Figure 5. Graph ln (V/Tp2) vs. 1000/Tp. - Kissinger method for the paraffin and paraffin/nanoparticle mixtures

Table 3. The activation energy, pre-exponential factor, and correlation coefficient

Sample	%wt. Fe_3O_4	Solid-Solid E_a (kJ/mol)	ln A	R	Solid-Liquid E_a (kJ/mol)	ln A	R
Np-0	0.00	377.26	151.51	0.93	705.08	262.70	0.97
Np-1	1.00	463.89	186.09	0.99	596.19	222.23	0.97
Np-5	5.00	480.09	192.67	0.97	791.87	294.49	0.95
Np-10	10.00	351.63	140.60	0.89	546.54	202.88	0.96

From Table 3 it can be noticed that the activation energy get an increasing on the solid-solid phase transition with increasing of Fe_3O_4loading, and maximum value indicated at 1wt.%of nanoparticles ratioalso decreasing in the values of E_a can be noticed at 1, 5and 10wt.% nanoparticle loading.On the other side the activation energy valueare decreased with the nanoparticles addition for the solid-liquid phase transition and increased gradually with increasing Fe_3O_4 loading, the maximum increasing found at5wt%nanoparticles.

4. Conclusions

In this paper, thermal behaviour ofFe_3O_4 nanoparticles enhanced paraffin wax were investigated. The nanomagnetite synthesized using chemical precipitation method with a diameter range 16.6-27.2 nm. The thermalbehaviour of paraffin/Fe_3O_4 were measured using DSC for three different ratio 1, 5 and 10wt%. The DSC results of latent heat showed a slight enhancement for 1wt% of nanoparticles loading, and decreasing in latent heat for the 5wt.%, and 10wt%.Sensible and latent heat of paraffin/Fe_3O_4 improved for the 1wt%, while no reasonable effect detected at 5wt.%. Specific heat capacity for solid and liquid phases recorded a decreasing for 10wt.%, and no significant variation observed for the other concentrations. Slight increasing in activation energy obtained at specific values 1and 5wt.% for solid-solid transition and 5wt.% for solid-liquid transition. The reason behind the thermal behaviour changes which occur due to nanoparticles using can be interpreted to the high surface area to the volume of the nanoparticles, and surface defect of the nanomagnetite caused by various coordination geometry. However at specific values of nanoparticles loading, Fe_3O_4 can be considered a promising candidate for thermal energy storage applications. More experiments should be achieved to detect the thermal conductivity behaviour and stability of Fe_3O_4in liquid phase of the mixture.

Acknowledgements

This work was supported by the Ministry of Science and Technology in Baghdad and by the Romanian National Authority for Scientific Research, Project PN II PCCA No 46/2014 and RO PN-II- RU-TE- 2014-4- 2412.

References

[1] H. Akeiber, P. Nejat, M. Z. A. Majid, M. A. Wahid, F. Jomehzadeh, I. Z. Famileh, J. K. Calautit, B. R. Hughes, Sh. A. Zaki, Renewable &Sustainable Energy Reviews **60**, 1470 (2016)
[2] B. Kanimozhi, A. Arnav, E. V. Krishna, R. Thamarai Kannan, Applied Mechanics and Materials **766-767**, 474 (2015)
[3] A. Sharma, V. V. Tyagi, C.R.Chen, D. Buddhi, Renewable & Sustainable Energy Reviews

13, 318 (2009)
[4] L. Min, Applied Energy **106**, 25 (2013)
[5] Y. Zeng, L. Fan, Y. Xiao, Z. Yu, K. Cen, International Journal of Heat and Mass Transfer **66**, 111 (2013)
[6] N. Jia, D. Ming, M. Yih, C. Yang, T. Niann, K. Chaur, W. Nen, Carbon **51**, 365 (2013)
[7] S.A. Angayarkanni, P. John, Physical Chemistry C **118**, 13972 (2014)
[8] W. Shuying, Z. Dongsheng, Z. Xiurong, H. Jin, Energy Fuels **24**, 1894 (2010)
[9] K Karunamurthy, K Murugumohankumar, S Suresh, Digest Journal of Nanomaterials and Biostructures **7**(4), 1833 (2012)
[10] C.J. Ho, J.Y. Gao, International Communications in Heat and Mass Transfer **36**, 467 (2009)
[11] C.J. Ho, J.Y. Gao, International Journal of Heat and Mass Transfer **62**, 2 (2013)
[12] S. Nurten, O. Halime, Solar Energy Materials & Solar Cells **126**, 56 (2014)
[13] Cem L Altan, SeydaBucak, Nanotechnology **22**, 285713 (2011)
[14] K. A. Gupta, M. Gupta, Biomaterials **26**, 3995 (2005)
[15] N. Sahan, H. O. Paksoy, Solar energy Materials & Solar Cells **126**, 56 (2014)
[16] J. A. Lopez, A.F Gonzalez, F. A. Bonilla, G. Zambrano, E. Gomez, Rev. Lat. Am. Metal. Mater. **30**, 60 (2010)
[17] V. Maria, A. PersisAmaliya, S, Vijayalakshmi, S. Pauline, International Journal of Technical Research and Applications e-ISSN: 2320-8163, 17 (2010)
[18] S. Y. Chazhengina, E. N. Kotelnikova, I. V. Filippova, S. K. Filatov, Journal of Molecular Structure **647**, 243 (2003)
[19] S. Shaikh, K. Lafdi, K. Hallinan, J. Appl. Phys **103**, 094302 (2008)
[20] Y. Cai, H. Ke, J. Dong, Q. Wei, J. Lin, Y. Zhao, L. Song, Y. Hu, F. Huang, W. Gao, H. Fong, Appl. Energy **88**, 2106 (2011)
[21] H. E. Kissinger, J. Analytical Chemistry **29**(11), 1702 (1957)